

ATLAS CONF Note Draft

CONF-FTAG-2017-02 Version 0.1

Comments are due by: DD Month 2017

Supporting internal notes

ATL-COM-PHYS-2017-192: https://cds.cern.ch/record/2253746

Calibration of light-flavour jet b-tagging rates on ATLAS proton-proton collision data at $\sqrt{s} = 13$ TeV

A variety of algorithms have been developed to identify jets originating from b-quark hadronization within the ATLAS experiment at the Large Hadron Collider. We describe two measurements of the misidentification rate of jets containing no b- nor c-hadrons for the algorithm most commonly used in the LHC Run 2 ATLAS analyses. The measurements are performed in various ranges of jet transverse momenta and pseudorapidities based on proton-proton collision data collected at a centre-of-mass energy of $\sqrt{s}=13$ TeV during the year 2015 and 2016. The first measurement is based on a data sample enriched in jets originating from light-flavour quark and gluon hadronization with the application of a dedicated algorithm reversing some of the criteria used in the nominal identification algorithm. The second measurement is based on a bottom-up approach where the underlying tracking variables in the simulation are adjusted to match the data. The effect is then propagated to the high-level observables relevant for b-identification. The results of both methods are found in good agreement and compared to the misidentification rate predicted by the nominal ATLAS simulation in order to calibrate it.

Analysis Team

[email: atlas-conf-ftag-2017-02-editors@cern.ch]

Valentina Cairo, Stefano Cali, Julian Glatzer, Emily Graham, Kristian Gregersen, David Jamin, Krisztian Peters, Matthias Saimpert, Balthasar Schachtner, Federico Sforza, Jonathan Shlomi

Editorial Board

[email: atlas-conf-ftag-2017-02-editorial-board@cern.ch]
Paolo Francavilla (chair), Claudia Gemme, Vadim Kostyukhin



11

12

13

14

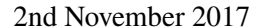
15

17

18

ATLAS CONF Note

CONF-FTAG-2017-02





Calibration of light-flavour jet b-tagging rates on ATLAS proton-proton collision data at $\sqrt{s} = 13$ TeV

The ATLAS Collaboration

A variety of algorithms have been developed to identify jets originating from b-quark hadronization within the ATLAS experiment at the Large Hadron Collider. We describe two measurements of the misidentification rate of jets containing no b- nor c-hadrons for the algorithm most commonly used in the LHC Run 2 ATLAS analyses. The measurements are performed in various ranges of jet transverse momenta and pseudorapidities based on proton-proton collision data collected at a centre-of-mass energy of $\sqrt{s} = 13$ TeV during the year 2015 and 2016. The first measurement is based on a data sample enriched in jets originating from light-flavour quark and gluon hadronization with the application of a dedicated algorithm reversing some of the criteria used in the nominal identification algorithm. The second measurement is based on a bottom-up approach where the underlying tracking variables in the simulation are adjusted to match the data. The effect is then propagated to the high-level observables relevant for b-identification. The results of both methods are found in good agreement and compared to the misidentification rate predicted by the nominal ATLAS simulation in order to calibrate it.

Reproduction of this article or parts of it is allowed as specified in the CC-BY-4.0 license.

Contents

21	1	Introduction	4
22	2	ATLAS detector	5
23	3	Data sample and event selection	6
24	4	Monte Carlo simulation	7
25	5	b-tagging algorithms	7
26	6	Track impact parameter modeling in the ATLAS simulation	8
27	7	Calibration with the negative tag method	8
28	8	Calibration with the adjusted Monte Carlo method	9
29	9	Comparison between the two methods	9
30	10	Conclusion	9
31	AI	ppendix	10
32	Αι	ıxiliary material	13

33 1 Introduction

The identification of jets originating from the hadronization of a *b*-quark (*b*-tagging) is an important element of a number of prominent analyses performed with the ATLAS detector [1] at the Large Hadron Collider (LHC): measurements of standard model processes aiming to constrain the heavy-flavour (HF) parton density functions [2], studies of the top quark [3] and of the Higgs-boson [4, 5], and exploration of New Physics scenarios [6, 7].

The b-tagging of a jet relies on the property of the b-hadrons to have long lifetime τ ($\tau \sim 1.5$ ps, corresponding to a proper decay length of about $c\tau \sim 450 \ \mu \text{m}$) and large mass, resulting in the production of tracks with non-zero impact parameters, secondary decay vertices and a large multiplicity of decay 41 products inside the jet cone. These observables are reconstructed with the help of the charged-particle 42 tracking capability of the ATLAS inner detector [8]. The information is then combined using a multi-43 variate algorithm able to enhance the discrimination of a jet containing b-hadrons (b-jet) with respect to a 44 jet containing no b-hadrons but c-hadrons (c-jet) or a jet containing no b-hadrons nor c-hadrons (LF-jet, LF standing for light-flavour). Specific selections on the output weight distribution of a given b-tagging algorithm are called working points (WP) and defined as a function of the average efficiency of tagging a b-jet as measured in a $t\bar{t}$ simulated sample [9, 10]. The algorithm most commonly used in the Run 2 ATLAS analyses is called MV2. It assigns to each jet a b-tagging weight ranging from -1 to 1. LF-jets and b-jets MV2 distribution peaks respectively towards -1 and 1, whereas the c-jets lie between the two. The 2016 version of MV2, which is the one considered in this document, is trained with a background sample including 7% of *c*-jets and 93% of LF-jets. It is denoted MV2c10 in the following.

The performance of a b-tagging algorithm [8] is characterised by the probability of tagging a b-jet (ε_b) and the probabilities of mistakenly tagging as a b-jet a c-jet (ε_c) or a LF-jet (ε_l), referred to as "mistag rates" in the following. Ideally, Monte Carlo (MC) simulations including the various quark flavours could be used to evaluate the b-tagging performance. However, additional calibration is often needed to account for differences between data and simulation, originating for instance from an imperfect description of the geometry of the detector. In practice, each working point of the algorithm is calibrated as a function of the jet transverse momentum ($p_T^{\rm jet}$) and absolute pseudorapidity ($|\eta^{\rm jet}|$). ¹

This document presents the measurements of the LF-jet mistag rate on ATLAS proton-proton collision data recorded at a center-of-mass energy of $\sqrt{s} = 13$ TeV for the MV2c10 WP listed in Table 1 using two methods giving consistent results, the negative tag and the adjusted MC. The negative tag method consists in measuring the LF-jet mistag rate from a high statistics data sample enriched in LF-jets with the application of a dedicated algorithm reversing some of the criteria used in the nominal identification algorithm. It was used previously in ATLAS in LHC Run 1 and Run 2 [11, 12]. The adjusted-MC method is a new calibration technique in ATLAS based on a bottom-up approach where the underlying tracking variables are adjusted to match the data and the effect is then propagated to the b-tagging observables. c-and b-jet performance are described in separate references [11, 13–15].

Table 1: *b*-tagging MV2c10 working points considered in this document. Each WP is defined by a cut value X on the MV2c10 output weight distribution (w > X, w ranging in [-1, 1]). The resulting b-tagging efficiency ($\varepsilon_b^{\text{MC}}$) and c- and LF-jet rejection rates ($1/\varepsilon_c$, $1/\varepsilon_l$) as measured in a $t\bar{t}$ simulated sample are also shown.

WP	Cut value X	$arepsilon_b^{ ext{MC}}$	c-jet rejection	LF-jet rejection
85%	0.18	85%	3	34
77%	0.65	77%	6	134
70%	0.82	70%	12	381
60%	0.93	60%	35	1539

9 2 ATLAS detector

The ATLAS experiment [1] at the LHC is a multi-purpose particle detector with a forward-backward symmetric cylindrical geometry and a near 4π coverage in solid angle. It consists of an inner tracking detector surrounded by a thin superconducting solenoid providing a 2 T axial magnetic field, electromagnetic and hadron calorimeters, and a muon spectrometer.

¹ ATLAS uses a right-handed coordinate system with its origin at the nominal interaction point (IP) in the centre of the detector and the *z*-axis along the beam pipe. The *x*-axis points from the IP to the centre of the LHC ring, and the *y*-axis points upwards. Cylindrical coordinates (r, ϕ) are used in the transverse plane, ϕ being the azimuthal angle around the *z*-axis. The pseudorapidity is defined in terms of the polar angle θ as $\eta = -\ln \tan(\theta/2)$. Angular distance is measured in units of $\Delta R \equiv \sqrt{(\Delta \eta)^2 + (\Delta \phi)^2}$. The transverse energy is defined as $p_T = E/\cosh(\eta)$.

The inner tracking detector (ID) covers the pseudorapidity range $|\eta| < 2.5$. It consists of silicon pixel, silicon micro-strip, and transition radiation tracking detectors. Among them, the pixel detector is crucial for *b*-jet identification. A new inner pixel layer, the Insertable B-Layer (IBL) [16, 17], was added before the start of Run 2, at a mean sensor radius of 3.2 cm from the beam-line.

Outside the ID, the lead/liquid-argon (LAr) sampling calorimeters provide electromagnetic (EM) energy measurements with high granularity. A hadron (iron/scintillator-tile) calorimeter covers the central pseudorapidity range ($|\eta| < 1.7$). The end-cap and forward regions are instrumented with LAr calorimeters for both EM and hadronic energy measurements up to $|\eta| = 4.9$. The muon spectrometer surrounds the calorimeters and is based on three large air-core toroid superconducting magnets with eight coils each. Its bending power is in the range from 2.0 to 7.5 T m. It includes a system of precision tracking chambers and fast detectors for triggering.

A two-level trigger system, using custom hardware followed by a software-based level, is used to reduce the event storage rate to a maximum of around 1 kHz.

3 Data sample and event selection

The proton-proton collision data sample recorded by the ATLAS detector during the year 2015 and 2016 is used. The LHC beams were operated with proton bunches organised in "bunch train", with a bunch spacing of 25 ns. Only events taken during stable beam conditions and satisfying detector and data-quality requirements are considered.

The data used in the measurements were recorded using a suite of single jet triggers [18], requiring in the event at least one hadronic jet with sufficient transverse energy $p_{\rm T}^{\rm jet}$ and absolute pseudorapidity $|\eta^{\rm jet}| < 3.2$. Hadronic jets are reconstructed from clustered energy deposits [19] in the ATLAS calorimeter with the anti- k_t algorithm [20] and a parameter R=0.4. Given the very high rates of such events at the LHC, only a fraction of events satisfying this requirement were recorded at low and medium $p_{\rm T}^{\rm jet}$ due to computational power and data storage limitations. In order to optimise the statistical power of the measurements, each $p_{\rm T}^{\rm jet}$ bin requires the trigger with lowest prescale (i.e. with highest integrated luminosity) that is more than 99.9% efficient in that range. The integrated luminosity of the data sample depends therefore on $p_{\rm T}^{\rm jet}$ and ranges from $0.02~{\rm pb}^{-1}$ (20 GeV $< p_{\rm T}^{\rm jet} < 60~{\rm GeV}$) to 36.1 fb⁻¹ (unprescaled, $p_{\rm T}^{\rm jet} > 500~{\rm GeV}$).

Events are required to have at least one reconstructed vertex with at least two associated well-reconstructed tracks. Futhermore, at least two jets reconstructed within the ATLAS inner detector pseudorapidity acceptance ($|\eta^{\rm jet}|<2.5$) passing cleaning criteria [21], identified as coming from the primary hard interaction [22] and satisfying $p_{\rm T}^{\rm jet}>20$ GeV after final calibration [23] must be present. If more than two jets satisfy these criteria, the two jets with the highest transverse momenta are selected and the others are disregarded. A good angular separation between the two jets in the transverse plane ($\Delta\phi_{jj}>2$ rad.) is also required in order to reject events with high transverse momentum jets originating from the hadronization of a gluon which split into two quarks ($g \to q\bar{q}$), more likely to contain c- and b-jets, or beam-induced background due to proton losses upstream of the interaction point [24].

² This condition cannot be achieved in the lower $p_{\rm T}^{\rm jet}$ category considered for the measurements (20 GeV < $p_{\rm T}^{\rm jet}$ < 60 GeV) such that a kinematical bias from trigger inefficiency is expected to affect the highest transverse momentum jets in data satisfying 20 GeV < $p_{\rm T}^{\rm jet}$ < 60 GeV. This issue will be discussed later in this note.

4 Monte Carlo simulation

Samples of inclusive dijet events from strong interaction processes are generated with Pythia 8.186 [25] MC generator with the NNPDF 2.3 LO parton distribution functions (PDFs) [26]. This generator utilizes leading-order perturbative quantum chromodynamics (pQCD) matrix elements for $2 \rightarrow 2$ processes, along with a leading-logarithmic parton shower [27], an underlying event (UE) simulation with multiple parton interactions, and the Lund string model for hadronisation [28]. The parameters for the modelling of the interaction features not represented by the matrix element are provided by the A14 tune [29]. Alternative samples of inclusive dijet events from strong interaction processes are generated with HERWIG++ 2.7.1 MC generator [30] with the CTEQ6L1 LO PDFs [31] and the UEEE5 tune for the modelling of the interaction feature not represented by the matrix elements (parton shower, hadronization, underlying event).

Generated events are propagated through a full simulation of the ATLAS detector [32] based on Geant4 [33] that simulates the particle interactions with the detector material. All generated events are part of the MC15c campaign, which was processed with the release 20.7 of the ATLAS software. Hadronic showers are simulated with the FTFP BERT model [34]. Different pileup conditions as a function of the instantaneous luminosity are taken into account by overlaying simulated minimum bias events generated with Pythia8 onto the hard-scattering process and reweighting them according to the distribution of the mean number of interactions observed in data.

Residual differences between data and simulation regarding jet cleaning requirement efficiencies are at the few percent-level and corrected by means of event-wide scale factors applied to the simulated events.

No corrections related to *b*-tagging performance are applied.

5 b-tagging algorithms

The identification of b-jets in the ATLAS experiment is based on a set of b-tagging algorithms relying on observables based on the reconstruction of signed track impact-parameters, signed secondary vertices, and decay chain multi-vertices. The output of the b-tagging algorithms is then combined into MV2c10, a multivariate discriminant trained on a background sample including 7% of c-jet and 93% of LF-jets for the optimal separation between b-jets and c-jets/LF-jets, with values ranging between -1 and 1. LF-jets (b-jets) MV2 distribution peaks towards -1 (1) whereas the c-jets lie between the two. A detailed description about all the tagging algorithms used in MV2 can be found in [9, 10]. They are described briefly below.

• Impact Parameter based Algorithms (IP2D and IP3D): due to long lifetime of *b*-hadrons, tracks generated from *b*-hadron decay products tend to have large impact parameters enabling their contribution to be separated from the contribution of tracks from the primary vertex. The IP2D and IP3D algorithms make use of the signed impact parameter significance of the tracks associated with the jet. The sign is defined positive (negative) if the point of closest approach of the track to the primary vertex is in front (behind) the primary vertex with respect to the jet direction. IP3D uses both the transverse and longitudinal impact parameters taking into account their correlations, while IP2D uses the transverse impact parameters only. The probability density functions (pdfs) for the signed impact parameter significance of these tracks are used to define ratios of the b, c and light-flavour jet hypotheses, and these are then combined in three log likelihood ratio discriminant (LLR): *b*/LF, *b*/*c* and *c*/LF.

- Secondary Vertex Finding Algorithm (SV1): SV1 aims to explicitly reconstruct an inclusive displaced secondary vertex within the jet. The first step consists of reconstructing two-track vertices using the candidate tracks. Tracks are rejected if they form a secondary vertex which can be identified as likely originating from the decay of a long-lived particle (e.g. K_s or Λ), photon conversions or hadronic interactions with the detector material. A new vertex is then fitted with all tracks surviving this selection, outlier tracks being iteratively removed from this set of tracks. The vertex information is condensed in the eight following observables: the invariant mass of tracks at the secondary vertex assuming pion masses, the fraction of the charged jet energy in the secondary vertex, the number of tracks used in the secondary vertex, the number of two track vertex candidates, the transverse distance between the primary and secondary vertices, the distance between the primary and secondary vertices divided by its uncertainty and the ΔR between the jet axis and the direction of the secondary vertex relative to the primary vertex.
- Decay Chain Multi-Vertex Algorithm (JetFitter): JetFitter exploits the topological structure of weak b- and c-hadron decays inside the jet and tries to reconstruct the full b-hadron decay chain. A Kalman filter is used to find a common line on which the primary vertex and the HF vertices lie, approximating the b-hadron flight path, as well as their positions. Hence, HF vertices can be resolved even when only a single track is attached to them whenever the resolution allows. The vertex information is condensed in the eight following observables: the number of 2-track vertex candidates prior to the decay chain fit, the invariant mass of tracks from displaced vertices assuming pion masses, the significance of the average distance between the primary and displaced vertices, the fraction of the charged jet energy in the secondary vertices, the number of displaced vertices with one track, the number of displaced vertices with more than one track, the number of tracks from displaced vertices with at least two tracks and the ΔR between the jet axis and the vectorial sum of the momenta of all tracks attached to displaced vertices.

₇₅ 6 Track impact parameter modeling in the ATLAS simulation

7 Calibration with the negative tag method

The negative tag method [12] relies to a large extent on the assumption that LF-jets are mistagged as *b*-jets mainly because of the finite resolution of the inner detector track impact parameters. Due to the long lifetime of *b*- and *c*-hadrons, the signed impact parameter distribution of the tracks associated with *b*- and *c*-hadron decays (i.e. within *b*- and *c*-jets) is expected to show a high tail at large positive values. This is the main discriminating feature used in impact parameter based *b*-tagging algorithms. Assuming that the LF-jet mistag is driven by resolution effects, the signed impact parameter distribution of the tracks associated with LF-jets, i.e. jets containing no *b*- nor *c*-hadrons, is expected to be symmetric. These properties are observed in simulated events, as shown in Figure ??. The inclusive tag rate obtained by re-running the MV2c10 algorithm after reversing the impact parameter significance sign of tracks is therefore expected to be a good approximation of the LF-mistag rate for impact parameter based algorithms. Moreover, the *b*-, *c*- and LF-jets impact parameter distributions being much more similar on the negative side than on the positive side (see Figure ??), one expects the inclusive negative tag rate to be comparable for the three flavors. Similar features are expected for the signed decay length significance of secondary vertices reconstructed with SV1 and JetFitter, which are seeded from tracks.

DRAFT

A dedicated tagging algorithm aiming to tag jets including negatively displaced tracks and negative lifetime secondary vertices, denoted MV2c10Flip in the following, is defined. It will be used as proxy to the LF-mistag rate. MV2c10Flip uses the same training and includes the same input variables as MV2c10, however the list of inputs variables is taken from modified versions of IP2D, IP3D, SV1 and JetFitter called respectively IP2DNeg, IP3DNeg, SV1Flip and JetFitterFlip, defined as follow:

- Negative Impact Parameter based Algorithms (IP2DNeg, IP3DNeg): only tracks with negative transverse impact parameter (d_0) are selected as inputs. The d_0 sign of the selected tracks is flipped before running the IP2D/IP3D algorithms. In the standard versions of IP2D/IP3D, both positive and negative d_0 tracks are used as inputs and no flipping is performed.
- Flipped Secondary Vertex Finding Algorithm (SV1Flip): the d₀ sign of the track used as inputs is flipped before running the SV1 algorithm. Once defined by the algorithm, only the two-track vertices with negative lifetime are considered to compute the output distributions. In the standard version of SV1, no flipping is performed and only two-track vertices with positive lifetime are considered to compute the output distributions.
- Flipped Decay Chain Multi-Vertex Algorithm (JetFitterFlip): the d₀ sign of the track used as inputs for two-track vertex reconstruction is flipped before the JetFitter algorithm. The sign of the two-track vertex candidates used to seed tracks for JetFitter is also flipped before running the rest of the algorithm. Once defined by the algorithm, only the final vertices with negative lifetime are considered to compute the output distributions. In the standard version of JetFitter, no flipping is performend and only final vertices with positive lifetime are considered to compute the output distributions.

A jet is then considered negatively tagged if the MV2c10Flip tag discriminant variable, ranging also between -1 and 1, satisfies the nominal WP cut value defined earlier in Table 1.

8 Calibration with the adjusted Monte Carlo method

9 Comparison between the two methods

10 Conclusion

196

197

198

200

201

203

204

205

206

207

208

209

211

217 Acknowledgements

The atlaslatex package contains the acknowledgements that were valid at the time of the release you are using. These can be found in the acknowledgements subdirectory. When your ATLAS paper or PUB/CONF note is ready to be published, download the latest set of acknowledgements from:

https://twiki.cern.ch/twiki/bin/view/AtlasProtected/PubComAcknowledgements

Appendix

In a paper, an appendix is used for technical details that would otherwise disturb the flow of the paper.
Such an appendix should be printed before the Bibliography.

225 References

- 226 [1] ATLAS Collaboration, *The ATLAS Experiment at the CERN Large Hadron Collider*, 227 JINST **3** (2008) \$08003.
- 228 [2] M. Aaboud et al., Measurement of differential cross sections of isolated-photon plus heavy-flavour jet production in pp collisions at $\sqrt{s} = 8$ TeV using the ATLAS detector, (2017), arXiv: 1710.09560 [hep-ex].
- [3] ATLAS Collaboration, Measurement of the $t\bar{t}$ production cross-section using $e\mu$ events with b-tagged jets in pp collisions at $\sqrt{s} = 7$ and 8 TeV with the ATLAS detector, Eur. Phys. J. C **74** (2014) 3109, arXiv: 1406.5375 [hep-ex].
- [4] M. Aaboud et al., Evidence for the $H \rightarrow b\bar{b}$ decay with the ATLAS detector, (2017), arXiv: 1708.03299 [hep-ex].
- 236 [5] ATLAS Collaboration, Search for the Standard Model Higgs boson produced in association with 237 top quarks and decaying into a $b\bar{b}$ pair in pp collisions at $\sqrt{s} = 13$ TeV with the ATLAS detector, 238 ATLAS-CONF-2017-076, 2017, URL: https: 239 //atlas.web.cern.ch/Atlas/GROUPS/PHYSICS/CONFNOTES/ATLAS-CONF-2017-076.
- [6] M. Aaboud et al., Search for a scalar partner of the top quark in the jets plus missing transverse momentum final state at \sqrt{s} =13 TeV with the ATLAS detector, (2017), arXiv: 1709.04183 [hep-ex].
- [7] ATLAS Collaboration, Search for heavy resonances decaying to a W or Z boson and a Higgs boson in the $q\bar{q}^{(\prime)}b\bar{b}$ final state in pp collisions at $\sqrt{s}=13$ TeV with the ATLAS detector, (2017), arXiv: 1707.06958 [hep-ex].
- [8] ATLAS Collaboration, *Performance of b-jet identification in the ATLAS experiment*, JINST 11 (2016) P04008, arXiv: 1512.01094 [hep-ex].
- [9] ATLAS Collaboration, Expected performance of the ATLAS b-tagging algorithms in Run-2, ATL-PHYS-PUB-2015-022, 2015, url: https://cds.cern.ch/record/2037697.
- 250 [10] ATLAS Collaboration, *Optimisation of the ATLAS b-tagging performance for the 2016 LHC Run*, ATL-PHYS-PUB-2016-012, 2016, URL: https://cds.cern.ch/record/2160731.
- 252 [11] ATLAS Collaboration,
 253 Calibration of the performance of b-tagging for c and light-flavour jets in the 2012 ATLAS data,
 254 ATLAS-CONF-2014-046, 2014, URL: https://cds.cern.ch/record/1741020.
- ATLAS Collaboration, b-tagging calibration plots in light-flavour jets from 2015+2016 data using the negative-tag method, FTAG-2017-002, 2017,
 URL: https://atlas.web.cern.ch/Atlas/GROUPS/PHYSICS/PLOTS/FTAG-2017-002.

DRAFT

- 258 [13] ATLAS Collaboration, *b-tagging calibration plots using dileptonic tt events produced in pp* collisions at $\sqrt{s} = 13$ TeV and a combinatorial likelihood approach, FTAG-2016-003, 2016, URL: http://atlas.web.cern.ch/Atlas/GROUPS/PHYSICS/PLOTS/FTAG-2016-003.
- 261 [14] ATLAS Collaboration, b-tagging efficiency calibration using a tag-and-probe technique with opposite-sign, different-flavour dileptonic tt events produced in pp collisions at $\sqrt{s} = 13$ TeV, FTAG-2017-001, 2017,
- URL: http://atlas.web.cern.ch/Atlas/GROUPS/PHYSICS/PLOTS/FTAG-2017-001.
- 265 [15] ATLAS Collaboration,
 266 b-tagging efficiency calibration from 2015+2016 data on lepton+jets tt events, FTAG-2017-003,
 267 2017, URL: http://atlas.web.cern.ch/Atlas/GROUPS/PHYSICS/PLOTS/FTAG-2017-003.
- 268 [16] ATLAS Collaboration, 'ATLAS Insertable B-Layer Technical Design Report', 269 tech. rep. CERN-LHCC-2010-013, CERN, 2010, 270 URL: https://cds.cern.ch/record/1291633.
- 271 [17] ATLAS Collaboration,
 272 Plots of b-tagging performance before and after the installation of the Insertable B-Layer,
 273 FTAG-2017-005, 2017,
 274 URL: https://atlas.web.cern.ch/Atlas/GROUPS/PHYSICS/PLOTS/FTAG-2017-005.
- 275 [18] ATLAS Collaboration, *Performance of the ATLAS Trigger System in 2015*, Eur. Phys. J. C **77** (2017) 317, arXiv: 1611.09661 [hep-ex].
- 277 [19] ATLAS Collaboration,
 278 Topological cell clustering in the ATLAS calorimeters and its performance in LHC Run 1,
 279 Eur. Phys. J. C 77 (2017) 490, arXiv: 1603.02934 [hep-ex].
- ²⁸⁰ [20] M. Cacciari, G. P. Salam and G. Soyez, *The Anti-k(t) jet clustering algorithm*, JHEP **04** (2008) 063, arXiv: 0802.1189 [hep-ph].
- 282 [21] ATLAS Collaboration,

 Selection of jets produced in 13 TeV proton—proton collisions with the ATLAS detector,

 ATLAS-CONF-2015-029, 2015, url: https://cds.cern.ch/record/2037702.
- ATLAS Collaboration, *Tagging and suppression of pileup jets with the ATLAS detector*, ATLAS-CONF-2014-018, 2014, url: https://cds.cern.ch/record/1700870.
- 287 [23] ATLAS Collaboration, Jet energy scale measurements and their systematic uncertainties in proton–proton collisions at $\sqrt{s} = 13$ TeV with the ATLAS detector, (2017), arXiv: 1703.09665 [hep-ex].
- 290 [24] ATLAS Collaboration, Characterisation and mitigation of beam-induced backgrounds observed 291 in the ATLAS detector during the 2011 proton–proton run, JINST 8 (2013) P07004, 292 arXiv: 1303.0223 [hep-ex].
- ²⁹³ [25] T. Sjostrand, S. Mrenna and P. Z. Skands, *A Brief Introduction to PYTHIA 8.1*, Comput. Phys. Commun. **178** (2008) 852, arXiv: **0710.3820** [hep-ph].
- ²⁹⁵ [26] R. D. Ball et al., *Parton distributions with QED corrections*, Nucl. Phys. **B877** (2013) 290, arXiv: 1308.0598 [hep-ph].
- ²⁹⁷ [27] R. Corke and T. Sjostrand, *Improved Parton Showers at Large Transverse Momenta*, Eur. Phys. J. **C69** (2010) 1, arXiv: 1003.2384 [hep-ph].

DRAFT

- 299 [28] B. Andersson, G. Gustafson, G. Ingelman and T. Sjostrand,
 200 Parton Fragmentation and String Dynamics, Phys. Rept. 97 (1983) 31.
- 301 [29] ATLAS Collaboration, *ATLAS Pythia8 tunes to 7 TeV data*, ATL-PHYS-PUB-2014-021, 2014, 302 URL: https://cds.cern.ch/record/1966419.
- ³⁰³ [30] J. Bellm et al., *Herwig++ 2.7 Release Note*, (2013), arXiv: 1310.6877 [hep-ph].
- J. Pumplin et al.,

 New generation of parton distributions with uncertainties from global QCD analysis,

 JHEP 07 (2002) 012, arXiv: hep-ph/0201195 [hep-ph].
- 307 [32] ATLAS Collaboration, *The ATLAS Simulation Infrastructure*, Eur. Phys. J. C **70** (2010) 823, arXiv: 1005.4568 [hep-ex].
- 309 [33] S. Agostinelli et al., GEANT4: A Simulation toolkit, Nucl. Instrum. Meth. A 506 (2003) 250.
- G. Folger and J. P. Wellisch, *String parton models in GEANT4*, eConf **C0303241** (2003) MOMT007, arXiv: nucl-th/0306007 [nucl-th].

2 Auxiliary material

In an ATLAS paper, auxiliary plots and tables that are supposed to be made public should be collected in an appendix that has the title 'Auxiliary material'. This appendix should be printed after the Bibliography.

At the end of the paper approval procedure, this information should be split into a separate document – see atlas-auxmat.tex.